Photoelectrochemical Hydrogen Production Using New Combinatorial Chemistry Derived Materials

Proceedings of the 2002 DOE Hydrogen Program Review
DOE Project # DE-FC36-01GO11092
PI: Eric W. McFarland

Sung Hyeon Baeck, Kyoung-Shin Choi, Anna Ivanovskaya, Thomas F. Jaramillo, Withana Siripala, Galen Stucky, and Eric W. McFarland

Department of Chemical Engineering
University of California, Santa Barbara, CA 93106-5080
805 893-4343; Fax: 805 893-4731
e-mail: mcfar@engineering.ucsb.edu

Abstract

The overall project objective is the development and application of combinatorial methods to discover an efficient, practical, and economically sensible material for photoelectrochemical production of hydrogen from water and sunlight. We are exploring a shift in the research paradigm from conventional serial chemical research to a combinatorial approach featuring a systematic and deliberate high-speed exploration of the composition-structure-property relationships of new metal-oxide based solid-state materials. By intelligent and rapid design, synthesis, and analysis of large diverse collections of potential photoelectrochemical materials in libraries we are attempting to discover new and useful energy producing materials as well as better understand fundamental mechanism and composition-structure function relationships of these materials. Since funding began in September 2001 we have remained on or ahead of schedule for milestone completion as outlined in the monthly reports. We have designed and built several prototype systems for automated electrosynthetic deposition of metal oxides including both parallel and serial systems. We now have developed direct cathodic routes to oxides of several metals including W, Ni, Nb, Ti, Fe, Cu, Co, Mo, Zn by stabilization with several ligand types and made preliminary studies with libraries which have shown general trends. Specific improvements in W doped with Ni, Pt, and Ru have been observed. Preliminary work on electrosynthesis of mesoporous WO_3 and TiO_2 films from a peroxo-stabilized electrolyte using ionic surfactants has not yet shown highly ordered materials, however, increases in photocurrent have been observed which we are attempting to explain. Finally, an important derivative of our work has been from libraries of pulsed electrodeposited Pt doped WO_3 whereby a new means of creating nanoparticles has been developed which show high activity for methanol oxidation without the poisoning problems of pure Pt electrodes.

Introduction

Despite more than 40 years of significant taxpayer subsidized research and development on hydrogen photosynthesis from water, the best photocatalytic materials have high production costs or poor lifetimes or low efficiencies. The most efficient systems rely on two photon processes (per useful electron/hole pair) in a semiconductor heterostructure with less than 15% efficiencies [1-3]. Even in an optimized reactor configuration, such systems would require a sun exposed area (@200 w/m^2) of approximately 300 km x 300 km to supply the 80 Quads (~10^{20} J) of power consumed in the United States each year. Dispersed homogeneous and heterogeneous photocatalytic systems are, at present, less efficient and the costs of separation of the mixtures of H_2 and O_2 simultaneously produced are prohibitive. At present, no photoelectrochemical material or material system exists to meet the target fuel price of under $15 /MBTU (~$1.70/kg H_2).

The attraction of photosynthetic hydrogen production is the fundamental thermodynamics of the water splitting reaction [4-5]. We share the hypothesis, which has driven past research in this field, that there exists an energetically and kinetically favorable photoelectrochemical process which can yield efficient and economical hydrogen photosynthesis. The failure to achieve success to date has not been due to lack of effort or intelligence; rather, it has been in the approach to identifying new material systems. All previous efforts in this field have relied on conventional chemical methods of making and testing materials one at a time and thus only a relatively few potential candidate material systems have been investigated out of countless possible choices. There is no theory that can predict in advance which composition and form of matter will give rise to the most efficient photocatalyst, and using conventional methods to try all possible combinations will take an extraordinarily long time and cost an exorbitant amount of money.

In our research we are utilizing a combinatorial approach to new materials discovery featuring a systematic and deliberate high-speed exploration of the composition-structure-property relationships of new metal-oxide based solid state material compositions and structures. Figure 1 illustrates our use of the combinatorial methodology in researching solid-state photocatalytic materials.

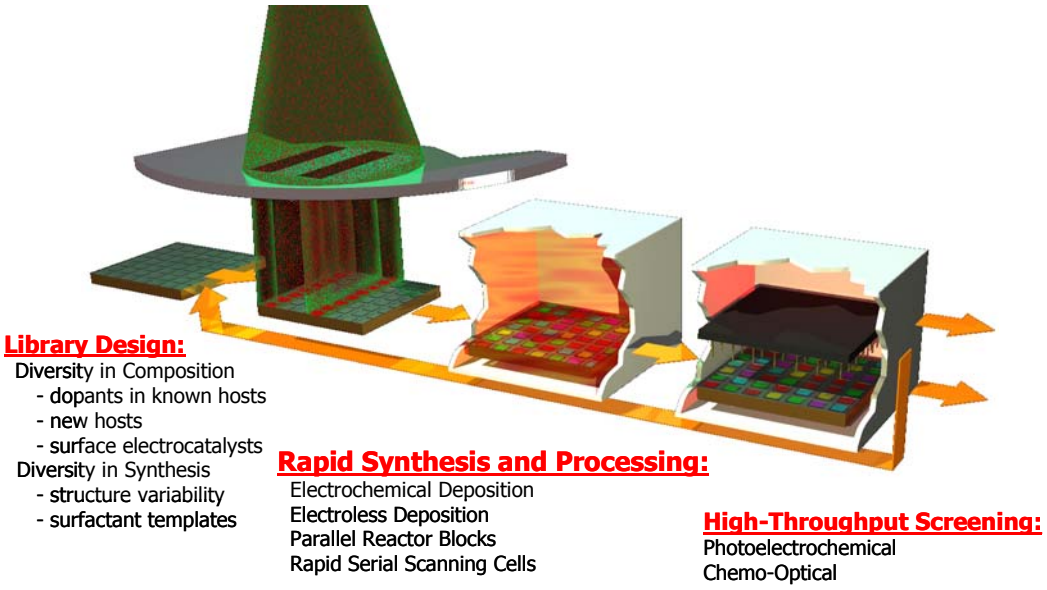

Fig. 1. The methodology of combinatorial material science as applied to this project.

By intelligent and rapid design, synthesis, and analysis of large diverse collections of potential photoelectrocatalytic systems (called "libraries"), we are working to discover new and useful energy producing materials as well as better understand fundamental mechanisms and composition-structure-function relationships of these materials. These methods and materials will have applicability not only to hydrogen photocatalysis but also to more general areas of material science related to energy.

The combinatorial methodology has been widely applied for new pharmaceutical discovery and more recently, to new inorganic materials discovery [6-9]. The preliminary studies described herein utilize electrochemical methods of combinatorial library synthesis and screening. Our results show that we can create diversity of composition electrochemically in several potential metal-oxide candidate photocatalyst systems. Our studies to date have focused on the development of automated systems, then on the preparation and analysis of diverse photoelectrochemical libraries of metal-oxides with semiconducting and other properties suitable for photoelectrocatalysis. Diversity is achieved by: (1) variations in composition (by variable doping, electrochemical synthesis conditions, and surface redox catalysts), and, (2) variations in structure (by deliberate and diverse ionic and non-ionic templating agents, synthesis conditions, and doping). The libraries are screened directly for hydrogen production using a two-dimensional chemo-optical sensor array. We also utilize high-throughput electrochemical and optical screening systems that can identify potential candidate materials before directly measuring H_2 production. New materials identified in the screening procedure as having a high likelihood of efficient performance are synthesized individually for detailed quantitative conventional analysis, characterization, and comparison with existing materials. Combinatorial methods are complementary to conventional chemistry and do not replace it!

Goals and Objectives

In working towards our ultimate goal of discovering and developing new, useful, and cost-effective materials for photocatalytic hydrogen production, we have addressed the Specific Aims outlined below:

1: Design and construct a versatile automated system and methodologies for automated electrochemical synthesis of combinatorial libraries of mixed metal oxides.

2: Define electrosynthetic routes amenable to the automated synthesis system for doped and mixed metal oxides which can be synthesized by automated electrochemical deposition.

3: Develop an automated high-throughput photoelectrochemical screening system for measuring electrochemical and photoelectrochemcial properties of the libraries.

4: Create and screen libraries of materials, which include well known oxides to validate the methodology by comparing observed performance trends to known behavior.

5: Complete the development of a chemo-optical detection system based on optical sensing of the reduction of tungsten oxide as a high-throughput screening system for monitoring.

6: Begin exploratory synthesis and screening of new metal-oxide systems and begin to examine composition-structure-function relationships and the relationship between screened properties and catalytic performance for hydrogen photocatalysis.

7: Design and synthesize libraries of potential patterned metal oxides using diverse types of structure directing agents (e.g. anionic and non-ionic surfactants, and block copolymers) under

a variety of deposition conditions to explore synthesis structure relationships for nanostructured metal/metal oxide thin films with accessible pores and high surface areas.

8: Specify database requirements for a large-scale combinatorial discover project and begin establishing appropriate data structures.

9: Synthesize and screen in year 1 at least three libraries and perform detailed conventional analytical studies to validate the electrochemical synthesis methodology.

The Progress Status section below discusses each Specific Aim in detail.

Progress Status

Specific Aim 1

Automated electrochemical synthesis routes will be used to create libraries of mixed metal oxides, and we have designed and constructed the necessary apparati and developed the detailed methodology to do so. We have examined the benefits and costs associated with parallel synthesis versus rapid serial synthesis and found that both are worthy of use in particular syntheses depending on the materials to be studied; we have engineered combinatorial synthesis systems of each kind. Specific issues addressed included speed, compositional control, and system cost. Figure 2 schematically illustrates how our synthesis systems operate. Figure 3 shows photographs of the actual systems.

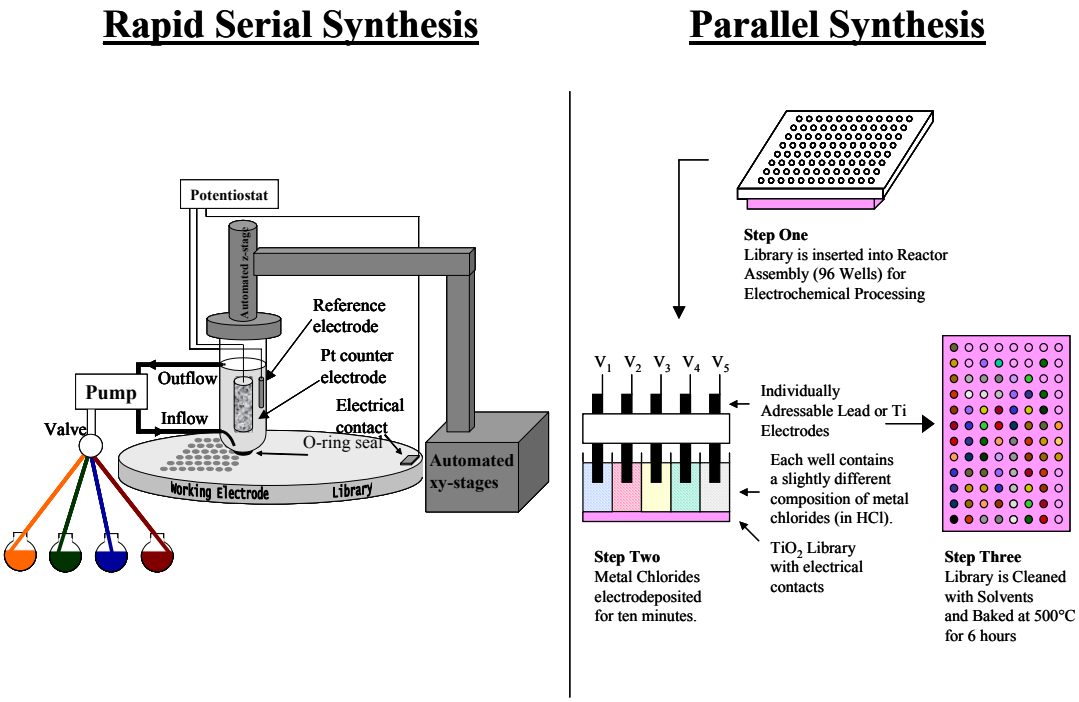

Fig. 2. Schematic illustration of combinatorial synthesis by electrochemical deposition. The parallel approach is faster, but the rapid serial method offers greater control for each deposition.

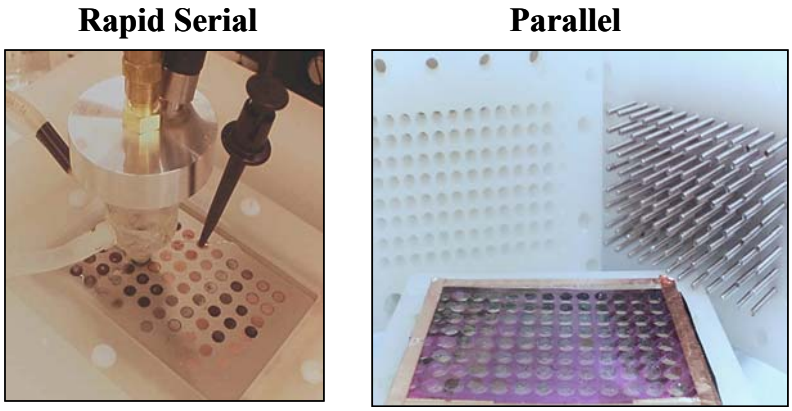

Fig. 3. Rapid serial and parallel electrochemical synthesis assemblies. The rapid serial approach involves a 3-electrode probe that is filled with electrolyte and moves spot-to-spot by means of an automated and computer controlled x-y-z stage. The parallelapproach utilizes 96 counter-electrode pins which can be multiplexed for truly parallel deposition.

Combinatorial methods only make sense when very large numbers of different materials are made and screened quickly. Compositional diversity across a library is obtained by varying the electrochemical deposition conditions of time, voltage, current, surfactant additives and electrolyte. In the parallel system, the substrate (which is a common working electrode) has individual electrochemical cells isolated from each other by virtue of a perforated polypropylene block that is sealed to the substrate with an array of o-rings. This provides for different synthesis conditions at each library position; each cell constitutes an individual two-electrode system and is filled with a compositionally unique electrolyte. Clearly, synthesis speed is the advantage in a parallel scheme since all depositions occur simultaneously. In the rapid serial system, a complete three-electrode probe is scanned over the surface of the library substrate by an automated, computer-controlled set of x-y-z stages. The probe contains an o-ring at the bottom which forms a seal at the substrate. Electrolyte of choice flows into the cell by a computer-controlled pump, and a highly controlled deposition is conducted at each location by an EG&G 273A potentiostat/galvanostat. Several material systems have exhibited extraordinary sensitivity to deposition voltage, and for these systems, the rapid serial approach is the only option due to its precise control. For other materials, however, the two-electrode parallel approach suffices, and hence the parallel approach is preferred for its speed.

Specific Aim 2

We have developed new electrochemical synthesis routes and extended existing ones to create routes amenable to our automated synthesis system for the generation of mixed metal oxides. The success of an electrosynthesis depends on the proper choice of a number of deposition parameters such as electrode material and geometry, electrolyte, temperature, pH, concentration and composition [10-12]. There are several routes for the synthesis of metal oxides by electrodeposition, as shown in Table 1.

Table 1. Electrochemical synthesis routes for metal oxides

Technique	Synthetic Route
Direct Metal oxide deposition	$2H_2O + 2e^- \rightarrow H^2 + 2(OH^-)_{sur}$ $M^{n+}(ligand) + n(OH^-)_{sur} \rightarrow M(OH)_nM(OH)_n \rightarrow MO_{n/2} + n/2\ H_2O$
Metal deposition and Post thermal annealing	$M^{n+} + n\ e^- \rightarrow M^o$ (Cathodic) $M^o + O_2 \rightarrow MO$
Anodization of metal	$M^o + H_2O \rightarrow MO + 2H^+ + 2e^-$

A number of metal hydroxides can be deposited by cathodic reduction. Metal oxides (WO_3, MoO_3, TiO_2, ZnO, Fe_2O_3, Co_3O_4…) can be produced from the metal hydroxide by thermal annealing. In some cases, metal (Ni, Zn, Mn,….) can be deposited by cathodic reduction and, after thermal annealing or electroanodization, a metal oxide can be obtained. We have used electrochemical anodization for the synthesis of Al_2O_3 to roughen the surface and create a porous base material [13].

Table 2. Precursors for the electrodeposition of metal oxides

Metal Oxides	Precursor
WO_3, MoO_3	Metal (W, Mo) + H_2O_2
Nb_2O_5, TiO_2	Metal Chloride ($TiCl_4$, $NbCl_5$) + H_2O_2
Cu_2O	Cupric Acetate + Sodium Acetate Cupric Chloride + Citric Acid Cupric Chloride + Lactic Acid
Fe_2O_3, Co_3O_4	Metal Sulfate or Chloride + H_2O

Our approach has been to stabilize the metal cations with ligands to allow for direct metal oxide deposition and the co-deposition of dopant cations. Several ligands we have used include hydrogen peroxide, citric acid, lactic acid, acetic acid. WO_3, TiO_2, Nb_2O_5, and MoO_3 have been cathodically deposited from metal-peroxo solution. We have found that mixed metal oxides, such as WO_3-MoO_3, WO_3-TiO_2 can be synthesized by mixing metal peroxo electrolytes. Pt or Ru doped tungsten oxide has been directly deposited under cathodic contitions in the presence of hydrogen peroxide and diversity has been achieved by changing the concentration of the dopants in the electrolyte solution or by varying deposition potential.

We have also stabilized the metal cations in basic media using a complexing agent such as citratic and lactic acid. Metal oxides, including Cu_2O, ZnO, FeO, and Fe_2O_3 have been deposited from metal-citrate, metal-lactate, or metal-acetate. We have also succeeded in the deposition of mixed oxides from these metal-ligand electrolytes.

Specific Aim 3

We have developed two principal systems for automated high-throughput photoelectrochemical screening designed to measure electrochemical and photoelectrochemical responses of combinatorially prepared photocatalyst libraries, Figures 4(a) and 4(b), respectively. The system in its electrochemical screening configuration allows for measuring cyclic voltammograms (I-V curves) and Mott-Schottky plots, which reveal flatband potential and sample dopant concentrations. The system is modular in nature – easy to set up for the experiment of interest by connecting the appropriate programmable source/measure devices: potentiostat, digital multimeter, data acquisition board, impedance analyzer and lock-in amplifier. This configuration allows for varying electrolytes for different samples by filling the wells of a perforated polypropylene block with a programmable pipette.

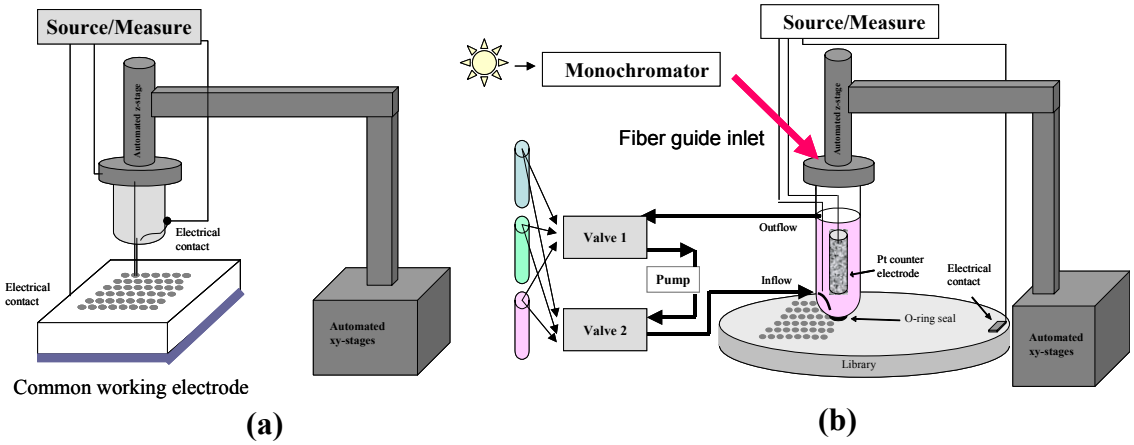

Fig. 4. High-throughput (a) electrochemical and (b) photoelectrochemical screening systems.

The system in its photoelectrochemical screening configuration allows for measuring photoresponse of photocatalyst libraries: photocurrent, photovoltage, photostability, and spectral response (which can be used to calculate bandgap). A specially designed probe is affixed to the motion stages to allow for such measurements. An o-ring is attached to the bottom of the probe to form a liquid seal with each library member. The probe contains a counter electrode, a reference electrode, ports for inflow and outflow of electrolyte, as well as a UV-transmissive light guide which targets the library sample. Each sample is illuminated by a 150W Xe lamp focused through the light guide. The source/measure devices employed include a potentiostat, digital multimeter, data acquisition board, and lock-in amplifier. The advantage of this system configuration is that there is no limitation on the library size, number, or geometry. A digital pump in combination with computer-controlled valves provide for electrolyte flow through the probe for measurement.

<u>IV Measurement</u>

The measurement of IV characteristics provide information on the semiconductor type and quality, flat band potential estimation, and the dependence of photocurrent upon applied bias. The following data, Figure 5, shows the improved photoresponse of copper oxide after thermal treatment.

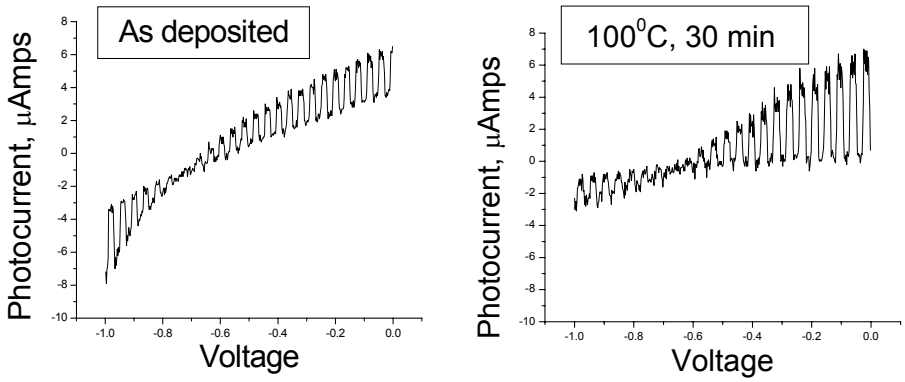

Fig. 5. The photocurrent of copper oxide improves after calcinations.

Mott-Schottky Plots

Under certain conditions, the space charge capacitance of a semiconductor obeys the Mott-Schottky equation, which allows one to calculate the flatband potential and doping level of the semiconductor. For the measurement of an interface capacitance, both DC (Potentiostat) and AC (Signal Generator) signals have to be applied, Figure 6(a). The imaginary component of the impedance, as measured by the lock-in amplifier, reveals information on capacitance.

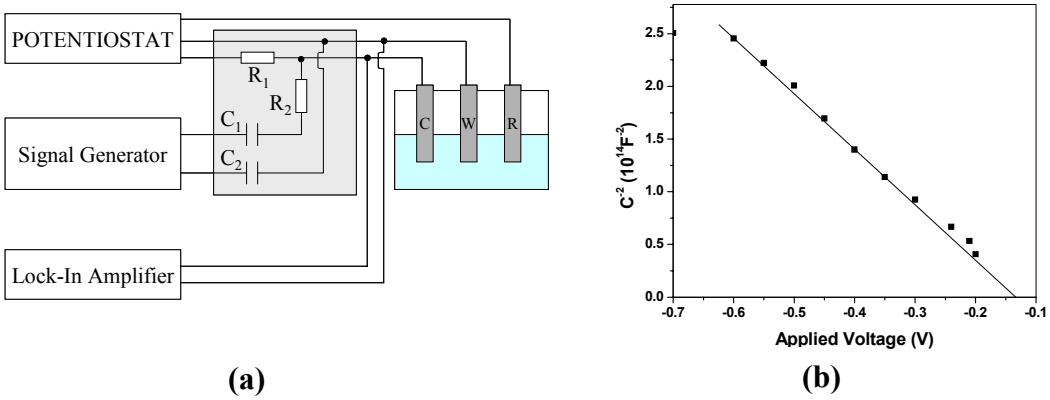

Fig. 6. (a) Schematic for the measurement of Mott-Schottky plots.
(b) Mott-Schottky plot for a Cu_2O sample.

As a function of the applied bias, the capacitance of the thin film semiconductor electrode in contact with the electrolyte is measured. A phase sensitive detection technique is employed to monitor the complex impedance of the interface at a fixed frequency. By plotting the resulting capacitance^{-2} vs. applied bias, one can obtain the doping density of the material and the flatband potential at the interface. Figure 6(b) shows a Mott-Schottky plot obtained for a thin Cu_2O film deposited on Au substrate in a 0.05 M cupric acetate solution at a potential of -0.4 V vs. Ag/AgCl. A doping density of 2.4×10^{17} cm^{-3} and a flat band potential of -0.13 V are obtained.

Spectral Response

Measuring the spectral response of semiconductor samples provides information on bandgap and on the quality of the materials and interfaces. The following spectra (Figure 7) were measured from copper oxide samples covered with different thin layers in order to improve the interface quality.

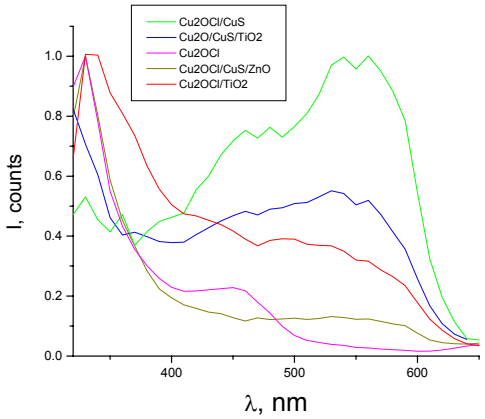

Fig. 7. Spectral response of a Cu_2O sample coated with different materials to improve photon absorption.

Specific Aim 4

Because WO_3 holds much promise as a host material for photocatalysis, we created a pair of libraries of WO_3 doped with different transition metals (at a variety of doping densities) with the aim of improving upon the photocatalytic activity of pure WO_3. The first library design is shown in Figure 8(a). The library incorporates Pt, Ru, Ni, Co, Cu, and Zn as dopants within polycrystalline WO_3. The materials were each co-deposited with WO_3 electrochemically from a mixture of 50mM metal chloride solution and a W-peroxo solution prepared by dissolving W metal powder in 30% hydrogen peroxide solution. Altering the metal-chloride concentrations in the electrolyte, from 0% to 50%, allowed for variation of doping concentrations within the deposited films. Figure 8(b) shows the relationship between doping density in the deposited film versus the concentration in the electrolyte for Pt and Ni as determined by Electron Dispersive X-Ray (EDX).

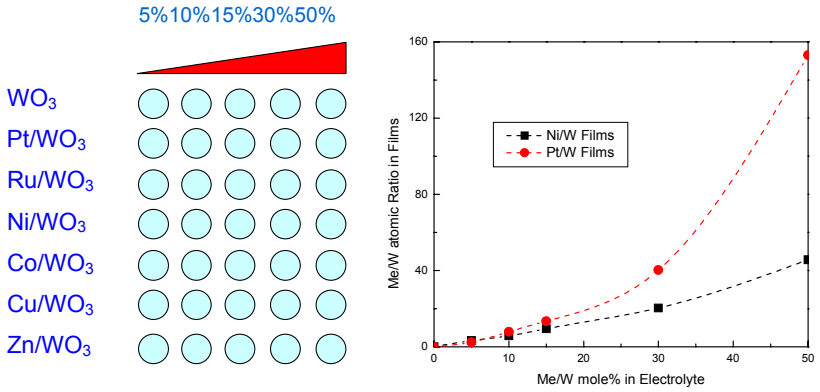

(a) **(b)**

Fig. 8. Metal-doped WO_3 binary library. (a) Library design: variation in doping density is achieved by varying dopant concentration in the electrolyte. (b) Relationship between dopant concentration in the deposited film versus dopant concentration in the electrolyte.

Figure 9(a) illustrates the zero-bias photocurrent for the library members, and Figure 9(b) shows a cyclic voltammogram taken of the pure WO_3 film. All samples were illuminated by a chopped 150 W Xe source and were immersed in 0.1M sodium acetate. Due to light intensity

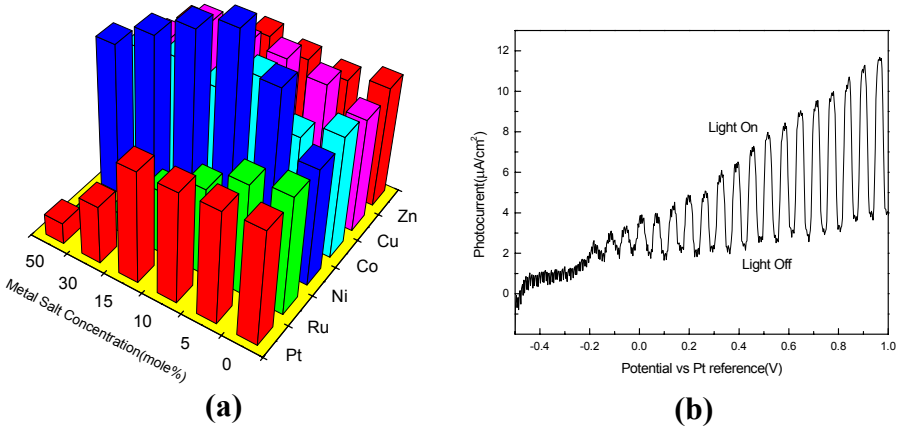

Fig. 9. High-throughput photocurrent screening of the WO_3 library at zero bias. (a) Photocurrent trends in the library. (b) Cyclic voltammogram of pure WO_3 (0.2 cm^2) under chopped illumination from a 150 W Xe lamp (2.3 mW/cm^2).

losses within the experimental setup, the light incident on the 0.2 cm^2 samples was only 2.3 mW/cm^2. We expect several photocurrent trends from this library. First of all, Ni has been shown to be an excellent absorber of visible light when doped into large band-gap oxide hosts, such as WO_3, so we expect an increase in photocurrent from that row. Similarly, we would expect better photocurrent from Pt and Ru dopants, since Pt is an excellent reduction catalyst and RuO_2 is a well-known oxidation catalyst. Figure 9(a) shows that, indeed, Ni doping increased photocurrent significantly compared to pure WO_3, with a maximum photocurrent achieved for 10% Ni. Pt and Ru dopants show a different trend. Seemingly, a greater doping concentration of either element decreases the photoactivity of WO_3. Judging from Figure 8(b), however, it is possible that too much of these dopants were deposited, altering the WO_3 too significantly to maintain its inherent photocatalytic activity. For this reason, a secondary WO_3 library was created, Figure 10.

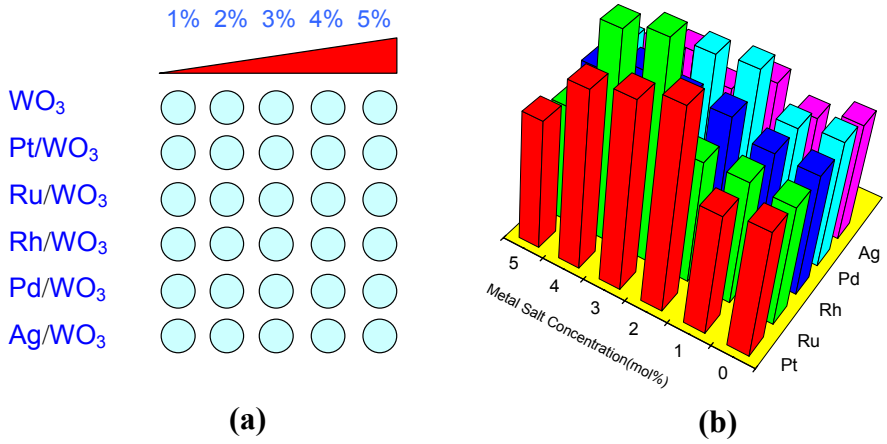

Fig. 10. Secondary metal-doped WO_3 library. (a) Library design: variation in doping concentration within the electrolyte was only 0%-5%, for greater resolution compared to the first WO_3 library. (b) Photocurrent trends.

The secondary WO_3 library was synthesized with a much smaller variation in doping concentration. The electrolyte varied from 0% to 5% dopant, as opposed to the 0% - 50% range used in the primary library. Photocurrent data for the second library can be found in Figure 10(b). With the greater resolution of this library, we can see that indeed, Pt and Ru improve upon the photocurrent of WO_3, but only in small concentrations. Since neither of these materials absorb light, adding too much of either most likely reduces photon absorption, and thus leads to lower photocurrent. A small doping density, however, benefits the catalytic properties of the surface without affecting photon capture, and hence, a greater photocurrent compared to pure WO_3 is observed.

Specific Aim 5

We have engineered a high-throughput screening system for monitoring H_2 production based on

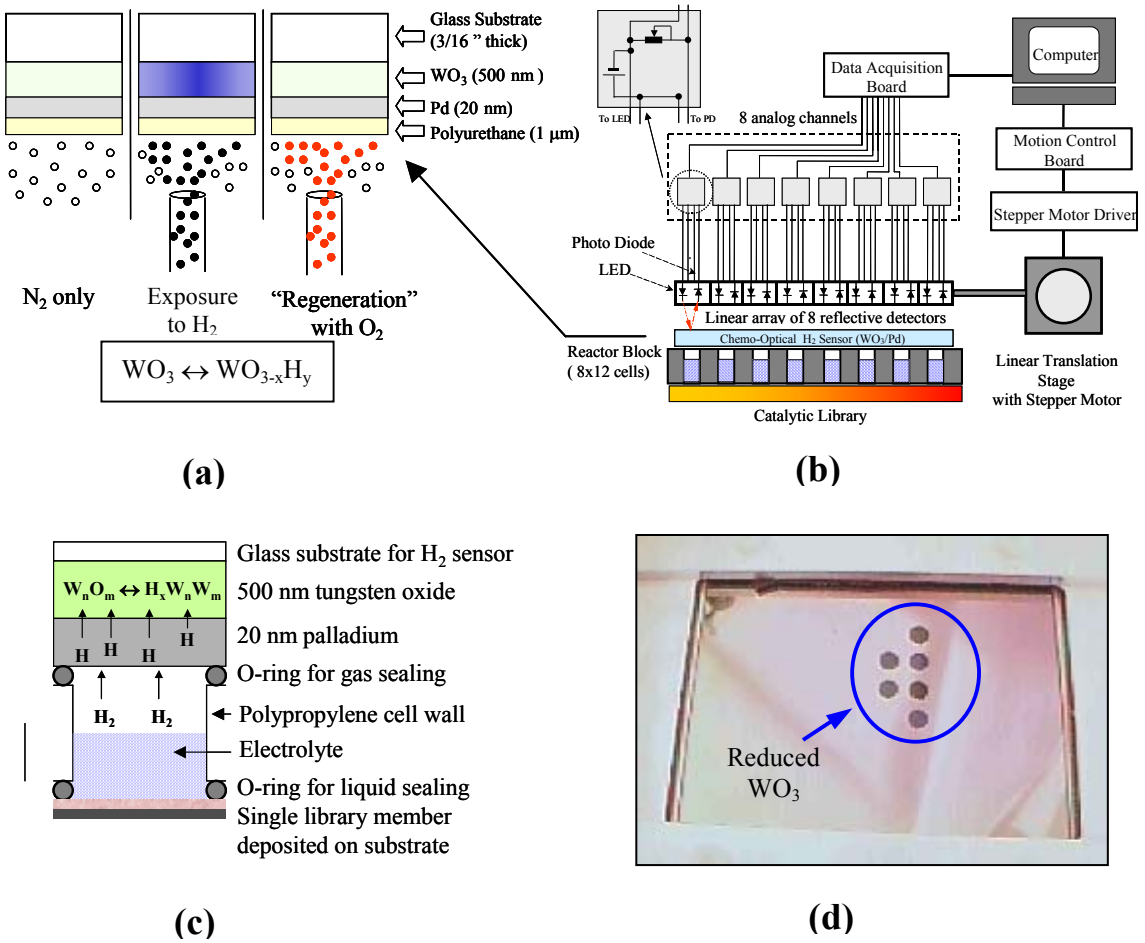

Fig. 11. Application of the WO_3/Pd H_2 sensor to high-throughput screening of H_2-producing materials (a) In the presence of H_2, the optical properties of the WO_3 layer change drastically. (b) By placing a perforated polypropylene "reactor block" over a library, one can form independent micro-reactors for each library sample. A large-area WO3/Pd sensor is sealed above the microreactors, and the reflectance of each spot is measured with an array of LEDs and photodiodes that are stepped across the library via computer-control. (c) Detailed schematic of a single micro-reactor in this scheme. (d) Actual photo of the sensor after screening. The blue spots indicate the materials of the library that produced H_2 at the greatest rate.

a chemo-optical H_2 sensor developed by Ito and Ohgami [14-16]. This colorimetric sensor utilizes a Pd/WO_3 bilayer whereby molecular H_2 dissociates on the Pd surface and diffuses as atomic hydrogen to reduce WO_3 to a tungsten bronze, H_yWO_{3-x}, Figure 11(a). The reduced tungsten oxide is photometrically distinct from WO_3 due to a decreased index of refraction; this effect is readily detected by changes in optical reflectance, and after significant reduction, the effect is clearly visible to the eye, Figure 11(d). The reduction is reversible and the sensor can be regenerated in O_2. We have extended the design of Ito and Ohgami for our large area multi-sample array applications in high-throughput screening of H_2 production.

Libraries of materials to be screened for H_2 production are deposited as thin films on glass or metal substrates in a 12 x 8 array. For high-throughput photocatalytic screening, a ½" thick polypropylene reactor block was constructed with 96 holes (7 mm diameter) designed to accept o-rings on both sides to form a gas/liquid sealed cell, Figure 11(b), and in more detail 11(c). One side of the polypropylene reactor block forms a liquid-seal with the library substrate, while the other side is gas-sealed to the Pd/WO_3 sensor. Each well is filled with approximately 200 mL of aqueous electrolyte for water-splitting. The 96 wells cover an area of 100 mm x 70 mm – dimensions slightly smaller than our large area, 2-D chemo-optical sensor.

In the high-throughput screening system, Figure 11(b), a linear array of small, commercial IR reflectivity sensors is used to map reflectance changes over the surface of the large area Pd/WO_3 film covering the library. Each reflectivity sensor package is about 200 mm^3 in volume and contains both a photodiode and an infrared light emitting diode (LED) operating at 935 nm. Eight sensor packages are assembled together to simultaneously measure the reflectance of 8 distinct, linear points on the Pd/WO_3 film. Using a linear translation stage driven by a stepper motor, the linear array is scanned repeatedly over the Pd/WO_3 film to achieve semi-parallel screening for H_2 production in a 96-well library; the reflectance measurements of all 96 members of the library are recorded every 30 seconds. The entire process of scanning and data acquisition is under software control (LabView™).

Specific Aim 6

The library shown in Figure 12 is a 45-member (5 x 9 array) WO_3-MoO_3 mixed binary oxide library, with diversity achieved by variations in deposition voltage and Mo concentration in the electrolyte. The library was deposited on a titanium foil. The concentration of Mo was varied from 0 to 100 mol% and all films were deposited for 10 minutes. After deposition, the library was calcined at 450 ^oC for 4 hours in air.

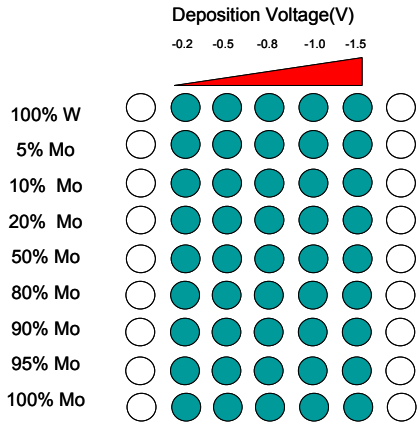

Fig. 12. Library design for WO_3-MoO_3 mixed oxide. Each electrolyte contained peroxo-stabilized tungsten with peroxo-stabilized molybdenum at various mole percentages for diversity.

The film compositions were determined by EDX for fifth row (prepared from 50% W- 50% Mo mixture) and 4th column (electrodeposited at –1.0 V). As expected, with increasing concentration of molybdenum in solution, the atomic fraction of molybdenum in the film increased (Fig. 13(a)). However, the atomic ratio was independent of deposition voltage (-0.2 ~ -1.5 V, not shown).

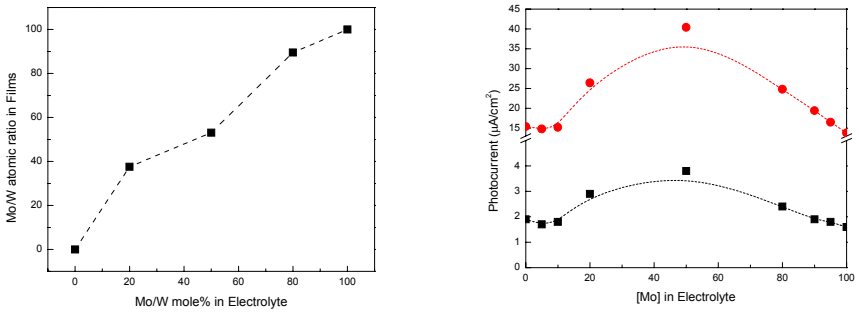

Fig. 13.(a) EDS measured atomic ratio of Mo to W in films as a function of Mo concentration in electrolyte. (b) Photocurrents in 0.1 M sodium acetate solution at zero bias(●)and 1 V bias(■) for WO_3-MoO_3 mixed oxides as a function of Mo concentration in electrolyte (4th column in library).

Automated photo-electrochemical screening of the library was performed. A trend in photoresponse as a function of molybdenum concentration in electrolyte was clearly observed. Figure 13(b) shows photocurrent at 0 and +1 V bias for the WO_3-MoO_3 mixed oxide. Photoactivity of the mixed oxides was strongly dependent on the film composition. The photoresponse increased and reached a maximum when 50% Mo and 50% W concentration in electrolyte was used, and then decreased as concentration of Mo in electrolyte increased. In the cases where MoO_3 concentration was below 10 % or above 90 %, there is no enhancement of photoactivity compared to either pure WO_3 or pure MoO_3. Interestingly, in the range of 20 ~ 80% MoO_3, an increase of photoactivity was observed.

Nano-particulate tungsten oxide films were synthesized by pulsed electrodeposition. Particle sizes between 45 ~ 330nm were achieved by varying pulse duration from 5 ms to 500 ms.

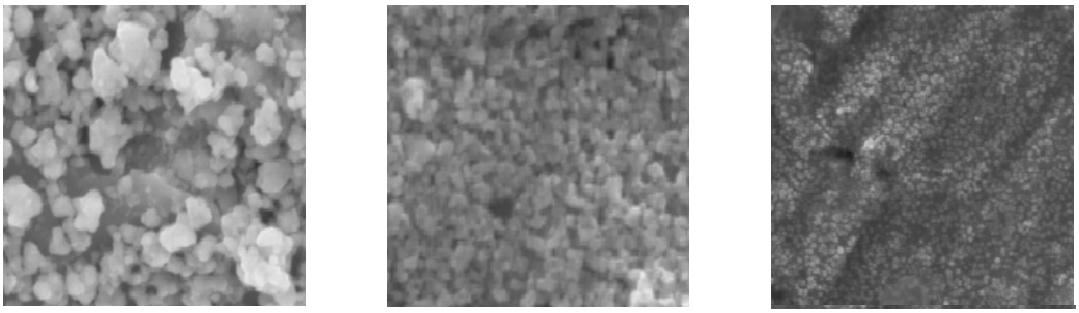

(a) **(b)** **(c)**

Fig. 14.Electron micrographs of tungsten oxide films prepared cathodically at –1 V by (a) normal continuous electrodeposition (b) pulsed deposition (100msec pulses) (c) pulsed deposition (5msec pulses)

Morphologies for several samples are shown in Figure 14. Films prepared by continuous electrodeposition had an average particle size of approximately 375 nm. As the pulse time decreased, particle size decreased as well, Figure 15. For a 5 msec pulsed deposition, the

average particle size was approximately 45 nm (Figure 14(c)). We checked the particle size with respect to deposition time (30sec to 30min, that is 3000 to 180,000 pulses) and found that particle size was independent of total number of pulses; the total number of pulses seemed to affect only film thickness and not the final particle size (not shown).

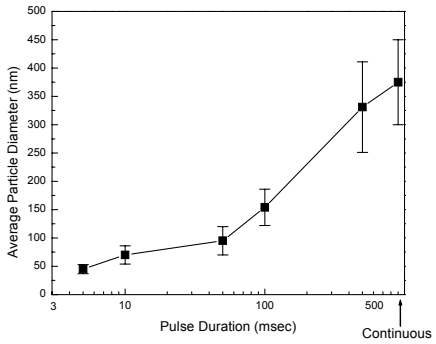

Fig. 15.Particle size as a function of pulse duration for WO_3 electrodeposition. Error bars indicate one standard deviation above and below the mean.

The growth of electrodeposited tungsten oxide films has been described as a 5 step nucleation-coalescence mechanism [17]: 1) formation of isolated nuclei, 2) growth to larger particles, 3) coalescence of larger particles, 4) formation of a linked network, and 5) formation of a continuous deposit. Smaller particle sizes can be explained by a higher nucleation rate with a decrease in the crystallite coalescence. Nucleation occurs at the instant the potential is switched on. Our results are consistent with a model whereby growth and coalescence of existing larger particles is less favorable that growth of the new small particle nuclei, thus during a single pulse cycle an individual particle is nucleated and grown to its maximum size.

Photoactivities for both continuous and pulse deposited films on ITO were measured under chopped illumination, Figure 16(a). The current-voltage behavior was typical of n-type semiconductor electrodes for all electrodeposited WO_3. In the case of films prepared by continuous electrodeposition, zerobias photocurrent (an indirect means of screening for

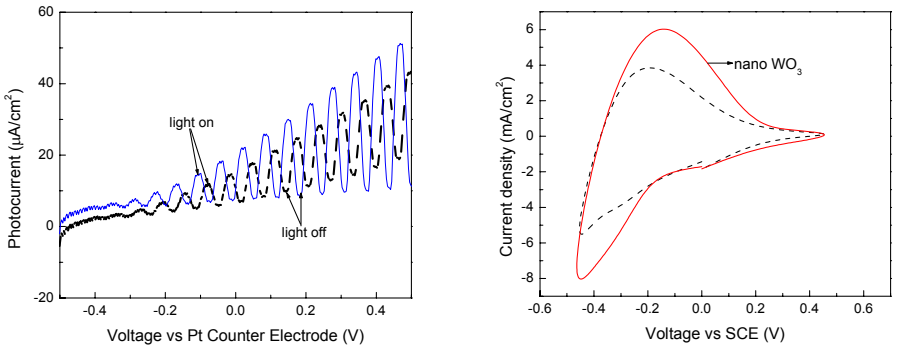

Fig. 16.Comparison of WO_3 prepared by pulsed electrodeposition and continuous electrodeposition. (a) Potentiodynamic scans under chopped illumination for tungsten oxide prepared by pulsed electrodeposition (solid line) and continuous electrodeposition (dashed line). The films were prepared on indium-tin oxide glass substrates. (b) Cyclic voltammogram for hydrogen intercalation/deintercalation in tungsten oxide films prepared by pulsed electrodeposition (solid line) and continuous electro-deposition (dashed line).

potocatalytic activity) increased with increased deposition time, and it reached a maximum value of approximately 8.5 ± 0.5 μA/cm^2 after 20 minutes of deposition. The photocurrent density of nano particulate tungsten oxide films was higher than that of the continuous WO_3 films and found to increase with decreased particle size.

When comparing the coloring current of tungsten oxides prepared by both pulsed and continuous electrodeposition, the nano crystalline tungsten oxide film on Ti foil shows significantly higher current density, Figure 16(b). This suggests that even though the films deposited continuously were thicker, for the same cathodic current, a lower potential can be used for the nano-crystalline tungsten oxide films. The improvement achieved in the hydrogen intercalation current and photoactivity can be explained by the significant increase of effective surface area due to the surface morphology and smaller particle size of nano-crystalline tungsten oxide.

We have discovered that metal oxides (WO_3, MoO_3, TiO_2, Nb_2O_5) can be synthesized from peroxo-stabilized solution onto Cu foil by electroless deposition. The deposition rate was found to be strongly dependent on temperature, electrolyte concentration, and deposition time. As-synthesized films were amorphous and showed weak p-type photocurrent due to the formation of Cu_2O on the surface of Cu foil. After calcination at 450°C, metal oxide films were found to be crystalline. The library shown in Figure 17(a) is a 27-member (3 x 9 array) WO_3-MoO_3 mixed oxide library prepared by electroless deposition on Cu foil, with diversity achieved by variations in deposition time and Mo concentration in electrolyte.

Current density for hydrogen intercalation was measured and a trend as a function of molybdenum concentration in electrolyte was clearly observed. Figure 17(b) illustrates the coloring current for the WO_3-MoO_3 mixed oxide, which was strongly dependent on the film composition. The current density increased and reached a maximum when an electrolyte consisting of 80% Mo and 20% W was used, and then decreased as concentration of Mo in electrolyte increased. Interestingly, in the range of 50 ~ 80% MoO_3, an increase of current density for hydrogen intercalation was observed, compared to either pure WO_3 or pure MoO_3.

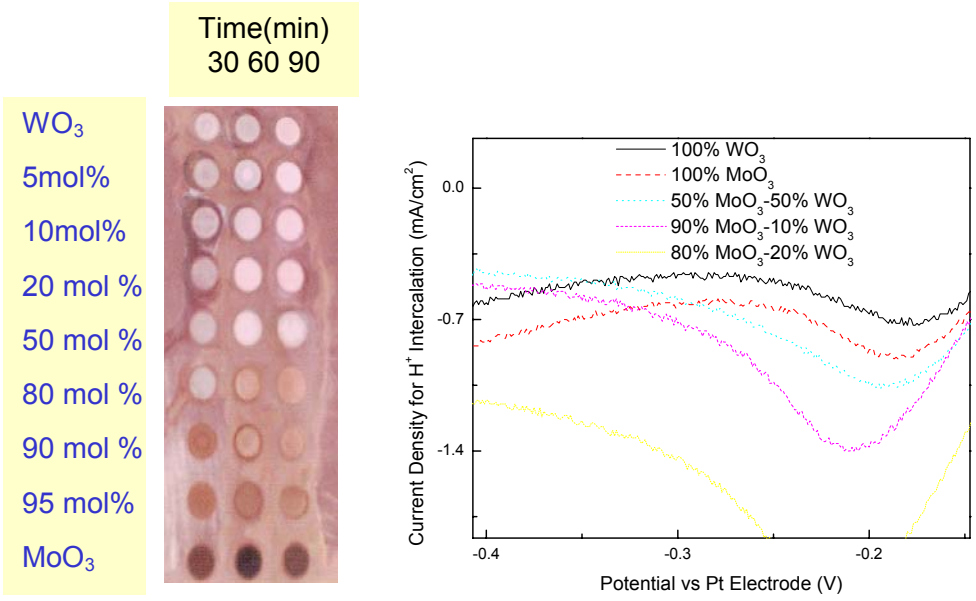

Fig. 17. WO_3-MoO_3 library prepared by electroless deposition on a Cu substrate. Library design: each electrolyte contained peroxo stabilized tungsten and peroxo-stabilized molybdenum at different mole percentages for diversity. (b) IV curves for hydrogen intercalation in the WO_3-MoO_3 mixed oxide films.

Specific Aim 7

In addition to our effort of finding better performance photocatalysts by tuning the composition of the films, we have been developing a general method for the production of high surface area nanostructured films by utilizing electrochemically driven self-assembly of surfactants at solid-liquid interfaces. The hope here is that by changes in morphology the accessibility of photon induced charges to reactant is increased. Surfactants in solution spontaneously aggregate at solid-liquid interfaces due to surface forces (i.e. electrostatic interaction between the surfactant head group and a surface charge). Micelles can be formed at the surface even when the surfactant concentration (surface micelle concentration, smc) is lower than the critical micelle concentration (cmc) because surface forces generate surface excess of surfactant molecules. The assembly patterns of the surface aggregates are frequently different from those formed in free solution. Among the factors that affect the organization of surfactants on the surface (i.e. hydrophilicity of the substrate, surfactant types, types of counter ions, and ionic strength), surface charge density is unique in that it can be controlled externally using a bias voltage applied to the substrate [18]. This makes it possible to selectively induce and stabilize phases of surfactant aggregates by deliberate control of the electrochemical potential.

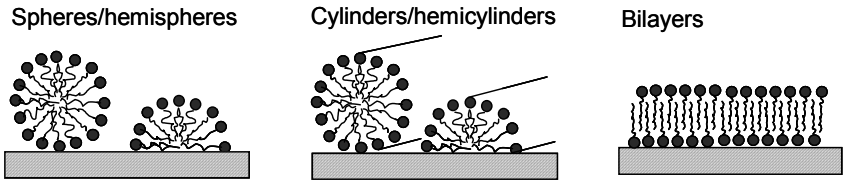

Fig. 18. Different surface assemblies of surfactants.

We combined potential-controlled surface assembly with an electrodeposition process to fabricate nanostructured films. In this approach, the surface of the working electrode serves as a solid-liquid interface in a plating solution containing surfactants. When there exists a common potential that can simultaneously induce a desired phase of surfactant-inorganic aggregates and reduce the metal ions, a nanostructured metallic film will be deposited patterned by the surfactant-inorganic aggregates. Figure 18 shows several surface assemblies of surfactants. Phases composed of hemisphere/sphere micelles and hemicylinder/cylinder micelles are suitable to fabricate mesoporous films (i.e. hexagonal, cubic, and disordered porous structures), while bilayers may result in layered structures or featureless films.

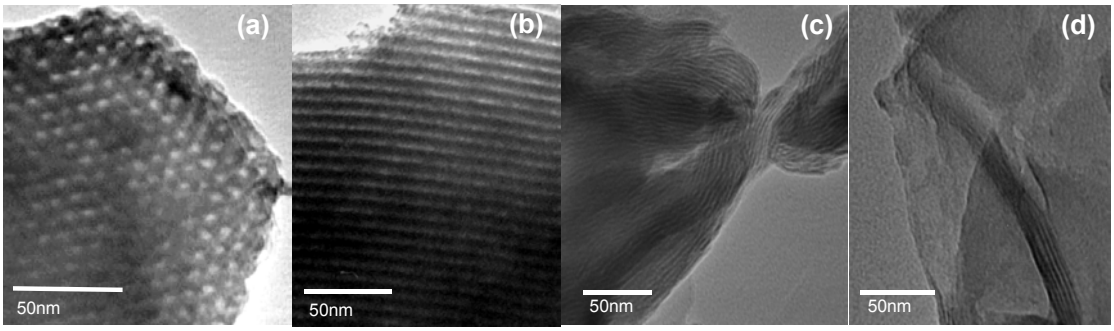

Fig. 19.TEM images of Pt films: (a) view of hexagonally ordered pores and (b) side view of pore channels. TEM images of ZnO film: (c) view of lamellar structure with the normal direction of the layers parallel to the substrate and (d) view of a flat region with thin ZnO sheets stacked perpendicular to the substrate.

Through this approach, we have successfully electrodeposited mesoporous platinum and zinc oxide films by controlling deposition potentials and electrolyte compositions. The nanostructures of these films confirmed by transmission electron microscopy (TEM) are shown

in Figure 19. The hexagonal structure of the Pt films with the pores perpendicular to the substrate (Figure 19(a)) and the lamellar structure of ZnO with the normal direction of the layers parallel to the substrate (Figure 19(c)) are expected to allow facile access of the guest molecules and analytes to the pores and interlayers.

The surface area of the mesoporous Pt film, which was determined using cyclovoltammetry, was estimated to be 47.1 m^2/g, which is equivalent to 1008 cm^3/m^2. For comparison, the specific surface areas of platinum black range from 20 to 28 m^2/g. The electrocatalytic properties of mesoporous Pt films towards methanol oxidation were measured in order to confirm the increased effective surface areas and to evaluate a potentially important application of these films (i.e. direct methanol fuel cell applications) (Figure 20).

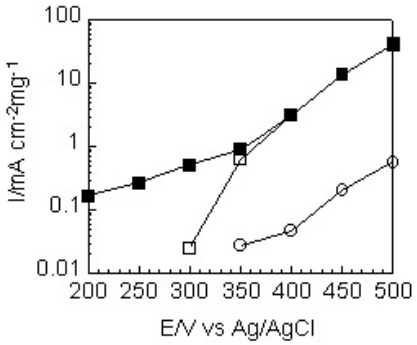

Fig. 20. Current densities for the oxidation of 0.5M methanol in 0.5M H_2SO_4 Recorded for several applied potentials after holding the potential constant for 2 minutes. (■) mesoporous Pt film, (□) electrochemically deposited Pt film without SS, and (○) Pt film deposited by electron beam evaporation.

The catalytic activity of the mesoporous Pt film for methanol oxidation was compared with those of the Pt film deposited by electron beam evaporation (~1.4 m^2/g) and the electrochemically deposited Pt film without SDS (~25 m^2/g). At low potentials, where the catalytic activity is critically determined by surface areas, the mesoporous Pt film shows significantly higher current densities compared to the other electrodes. Below 0.3V, only the mesoporous film shows noticeable catalytic activities. These results suggest that the walls of the porous structure are electrochemically active and act as effective catalytic sites. At higher potentials ($\geq$ 0.4V), the mesoporous film and the electrochemically deposited Pt film without SDS, show comparable performances because the rate of methanol oxidation becomes diffusion limited and all reactants reaching the surface is consumed on both surfaces such that no advantage is obtained from the presence of the pores.

These results prove that our method can generate nanostructured metallic and semiconducting films with high surface areas and accessible pores. We are currently extending our approach to the production of a variety of metal oxide films (i.e. WO_3 and TiO_2), which are more directly relevant to photocatalysis applications. We expect that our combinatorial approach will make it possible to rapidly find optimum synthetic conditions for each material type by deliberately exploring deposition conditions (e.g. deposition potentials, surfactant types and concentration, pH) and screening resulting photocatalytic properties.

Specific Aim 8

In combinatorial chemistry, the quantity of data collected is enormous. Our work in specifying database requirements for our large scale combinatorial discovery project has begun and is in progress. We expect to complete the specifications by the end of year 1.

Specific Aim 9

It is our goal to synthesize and screen by the end of the first 12 months at least three large libraries and perform detailed conventional analytical studies on selected samples to fully validate our electrochemical deposition methodology as a reliable and reproducible means of material synthesis on libraries. Most of our work to this point has involved developing the routes and tools necessary to accomplish this goal, and we are progressing on schedule to complete this aim.

Summary

Photoelectrocatalysis is a multi-factorial process which may have significant impact on future hydrogen production if efficient and economic materials can be found. At present the structure function relationships of photocatalysts are largely unknown and we believe combinatorial methods may be a means of increasing our rate of discovery and (possibly) understanding of new photocatalysts applicable to hydrogen production. Our work during the first 9 months of this project has focused on the development of combinatorial methods to rapidly synthesize and high-throughput screen mixed metal oxides, and on using these systems to begin to investigate new materials for photocatalytic hydrogen production. We have designed and constructed much of the combinatorial infrastructure (automated parallel and rapid serial synthesis and screening systems), and we have developed synthesis routes (based on electrochemistry) amenable to our combinatorial instruments. Rapid synthesis and functional screening of mixed metal oxides of W, Cu, Ti, and Fe hosts has been demonstrated and a new electrosynthetic routes to W-Mo-oxide and nanoporous WO_3 have been developed. Recent data from $W_x(Mo,Ni,Pt)_yO_z$, $Cu_x(Zn_yNi_y)O_z$ and $Fe_x(Ti)_yO_z$ show (reserved) promise as improved materials. Consistent with the combinatorial methodology, our future work will be guided by the leads we discover as we rapidly create and screen thousands of photocatalytic materials.

Publications and Presentations

(1) S.H. Baeck, T.F. Jaramillo, C. Brandli, and E. McFarland, “Combinatorial Electrochemical Synthesis and Characterization of Tungsten-based Mixed Metal Oxides”, J. Combi. Chemistry, (submitted 2002).

(2) S.H. Baeck, T.F. Jaramillo, G.D. Stucky, and E. McFarland, “Controlled Electrodeposition of Nanoparticulate Tungsten Oxide”, Nano Letters, (accepted and in press 2002).

(3) S.H. Baeck and E. W. McFarland, "Combinatorial Electrochemical Synthesis and Characterization of Tungsten-Molybdenum Mixed Oxides", Korean.J.Chem.Eng., (accepted and in Press 2002).

(4) S.H. Baeck, T.F. Jaramillo, and E. McFarland, ”Influence of composition and morphology on photo and electrocatalytic activity of electrodeposited Pt/WO_3”, 224th National ACS Conference proceedings, Boston, MA (2002).

(5) Invited Seminar October 2001 “Combinatorial Methods of New Materials Discovery For Photocatalytic Hydrogen Production: A Long Way to a Million Million Watts”, Department of Nuclear Engineering, MIT.

(6) Invited Talk November 2001 “Combinatorial Electrosynthesis and Photoelectrocatalytic Screening of New Materials For Hydrogen Photosynthesis”, AICHE Annual Meeting, Reno, Nevada.

References

1. Gaffron, H and Rubin, J., *J. Gen. Physiol.*, **26**, 219 (1942).
2. Fujishima, A. and Honda, K, *Nature*, **238**, 37 (1972).
3. Herriman, A. and West, M. A., editors, "Photogeneration of Hydrogen", Royal Institution Symposium, Academic Press (1982).
4. Domen, K., Kondo, J. N., Hara, M., and Takata, T., *Bull. Chem. Soc. Jpn.*, **73**, 1307 (2000).
5. Gratzel, M. A., "Energy Resources through Photochemistry and Catalysis", Academic Press, New York (1983).
6. Hanak, J. J., *J. Mater. Sci.*, **5**, 964 (1970).
7. Hanak, J. J., Gittleman, J. I., Pellicane, J. P., and Bozowski, S., *Phys. Lett.*, **30(3)**, 210 (1969).
8. Danielson, E., Golden, J. H., McFarland, E. W., Reaves, C. M., Weinberg, W. H., and Wu, X. D., *Nature*, **389**, 944 (1997).
9. Danielson, E., Devenney, M., Giaquinta, D. M., Golden, J. H., Haushalter, R. C., McFarland, 10. E. W., Poojary, D. M., Reaves, C. M., Weinberg, W. H., and Wu, X. D., *Science*, **279**, 837 (1998).
10. Therese G. H. A. and Kamath, P. V., *Chem. Mater.*, **12**, 1195 (2000).
11. Meulenkamp, E. A., *J. Electrochem. Soc.*, **144**, 1664 (1997).
12. Hutchins, M. G., Kamel, N. A., El-Kardy, W., Ramadan, A. A., and Abdel-Hady, K., *Phys. Stat. Sol. A* ,**175**, 991(1999).
13. Brandli, C., Jaramillo, T. F., Ivanovskaya, A., and McFarland, E. W., *Electrochimica Acta*, **47**, 553 (2001).
14. Ito, K. and Ohgami, T., *Appl. Phys. Lett.*, **60**, 938 (1992).
15. Ito, K. and Kubo, T., *Proceedings of the 4th Sensor Symposium*, Tokyo, 153 (1984).
16. Tamura, H., Hashimoto, Y., and Ito, K., *Solid State Phenom.*, **51-52**, 429 (1996).
17. Shen, P., Chi, N., and Chan. K. Y., *J. Mater. Chem.*, **1**, 697 (2000).
18. Burgess, I., Jeffrey, C. A., Cai, X., Szymanski, G., Galus, Z., and Lipkowski, J., *Langmuir*, **15**, 2607 (1999).